Chapter 5

In Situ Observation of Chemical Vapour Deposition Using Langasite Crystal Microbalance

Hitoshi Habuka

Additional information is available at the end of the chapter

http://dx.doi.org/10.5772/62389

Abstract

A method of *in situ* observation using langasite crystal microbalance (LCM) is described for chemical vapour deposition (CVD). First, the frequency behaviour of the LCM is expressed using the equation having the optimized coefficients in a wide range of gas-phase conditions for the CVD. Next, by the LCM frequency behaviour, the existence of surface chemical reactions in a CVD reactor is determined. Additionally, the LCM can determine the lowest temperature for initiating the film deposition. In the last part, the temperature change related to the film formation process is described.

Keywords: Chemical vapour deposition, *In situ* observation, Langasite crystal microbalance, Surface reaction, Gas properties

1. Introduction

Chemical vapour deposition (CVD) is currently a fascinating technology for producing thin films in various advanced industries [1]. The CVD process is a complicated one having transport phenomena linked with the gas-phase and surface chemical reactions. For clarifying and designing the CVD process, the phenomena in the CVD reactor should be understood and optimized. For this purpose, the computational fluid dynamics (CFD) has been significantly advanced [2] and is actually very useful. In contrast, an experimental approach is still not easy [3], because the sensors seriously suffer from thermal, mechanical and chemical damage by the reactive and high-temperature ambient.

The *in situ* monitoring technique by means of the langasite crystal microbalance (LCM) [4–6] can be an appropriate experimental solution, because the LCM can sensitively detect various

changes in the CVD reactor, such as heat, flow and film deposition [5, 6]. The information obtained by the LCM should be used for understanding the CVD phenomena. Here, the LCM frequency nonlinearly influenced by various parameters should be clarified. Additionally, a practical process for the measurement and analysis should be developed. In this chapter, the process to *in situ* observe the CVD is thus explained using the LCM.

In Section 1, the frequency behaviour of the LCM is discussed using ambient gas mixtures at atmospheric pressure and at various temperatures. In order to express the LCM frequency decrease with the increasing concentrations of various gases in ambient hydrogen, the LCM frequency difference between the gas mixture and the carrier gas is practically expressed by optimizing the coefficients accounting for the gas properties. In Section 2, a method for determining the existence of surface chemical reactions is explained. The parameter, $C(T)$, of the equation is used for expressing the LCM frequency change in a hydrogen–monomethylsilane system. In Section 3, the lowest temperature for initiating the film deposition is evaluated using trichlorosilane gas and boron trichloride gas. In Section 4, the way to obtain the temperature change related to the film formation in a trichlorosilane–hydrogen system is described. First, the time constants for the LCM frequency change due to the surface and gas-phase temperature change are determined. Next, the continuous LCM frequency decrease is assigned to the weight increase by the film formation in a steady state. Based on an evaluation of the difference in the LCM frequency between those with and without the heat change related to the film formation, the surface temperature decrease caused by changing the precursor concentration is obtained.

2. Langasite crystal microbalance frequency behaviour over wide gas-phase conditions for chemical vapour deposition

In this section, a relationship between the LCM frequency and the gas properties is expressed [7] as a practical equation applicable to the CVD conditions using several gases at various temperatures and gas concentrations.

2.1. Experimental procedure

Figure 1 shows the horizontal cold wall CVD reactor containing the langasite ($La_3Ga_5SiO_{14}$) crystal microbalance (LCM) [4, 8]. This reactor consists of a gas supply system, a rectangular-shaped quartz chamber and five infrared lamps. Hydrogen, nitrogen, trichlorosilane, monomethylsilane and boron trichloride gases are used. The carrier gas is hydrogen. The LCM (Halloran Electronics, Tokyo, Japan) having a fundamental frequency of 10 MHz is placed 5 mm above the silicon wafer surface. The LCM frequency decreases with the increasing temperature [5, 6]. The silicon wafer and the LCM are simultaneously heated by infrared light from halogen lamps through the quartz chamber.

A typical process is shown in **Figure 2**. First, the LCM is heated to 160–600°C in hydrogen at atmospheric pressure. After waiting until the LCM frequency becomes stable, various gases

http://dx.doi.org/10.5772/62389

are introduced at atmospheric pressure into the reactor chamber. The total gas flow rate is adjusted to 1 slm.

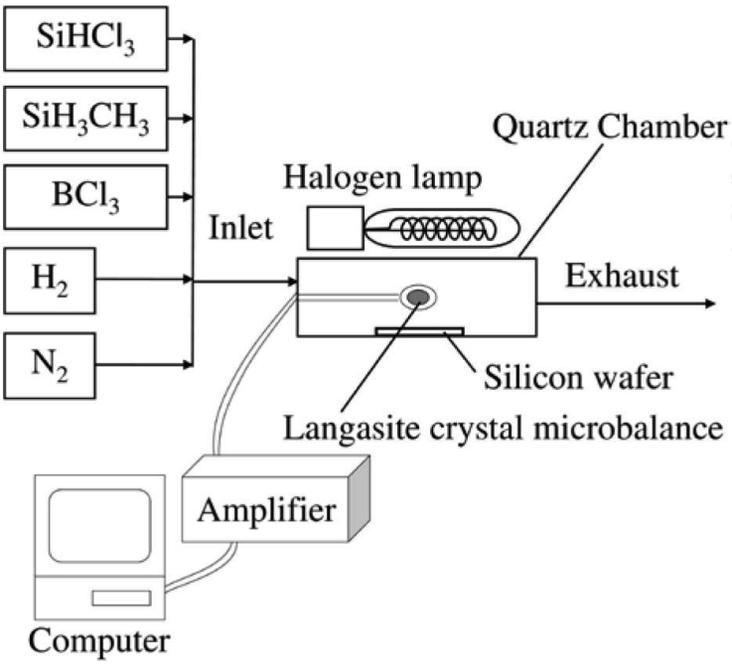

Figure 1. Chemical vapour deposition reactor containing a langasite crystal microbalance.

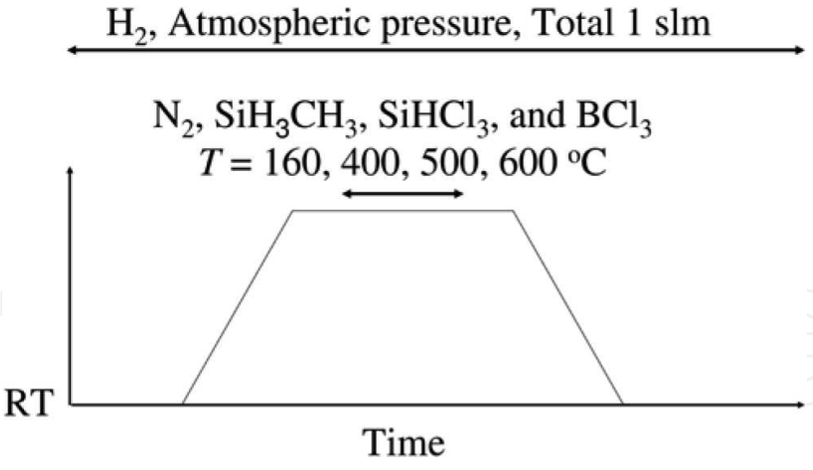

Figure 2. Process for measuring the frequency of the langasite crystal microbalance under various conditions.

2.2. LCM frequency and fluid property

The relationship between the LCM frequency and the gas properties is described, accounting for the various relationships shown in **Figure 3**. Following a previous paper [9], the LCM frequency change, Δf_{Gas}, at a fixed temperature, T (K), is expressed using the product of the gas density, ρ_{gas}, and gas viscosity, η_{Gas} as follows:

$$\Delta f_{\mathrm{Gas}} = -C(T)\rho_{Gas}^{y}\eta_{Gas}^{z}, \tag{1}$$

$$C(T) = \left(\frac{f_C^x}{\pi\rho_C^y\mu_C^z}\right) \tag{2}$$

where f_c is the resonant frequency of the fundamental mode of the langasite crystal. ρ_c and μ_c are the density and shear modulus, respectively, of the langasite crystal. Based on Kanazawa et al. [9], the x, y and z values are 1.5, 0.5 and 0.5, respectively. In a vacuum, the Δf value becomes zero.

The LCM frequency change from the vacuum condition to the hydrogen and to the gas mixtures are shown in **Figure 3** and are expressed by Eqs. (3) and (4).

$$\Delta f_{\mathrm{H_2}} = -C(T)\rho_{\mathrm{H_2}}^{y}\eta_{\mathrm{H_2}}^{z} \quad \text{(in hydrogen).} \tag{3}$$

$$\Delta f_{\mathrm{Mix}} = -C(T)\rho_{\mathrm{Mix}}^{y}\eta_{\mathrm{Mix}}^{z} \quad \text{(in gas mixture).} \tag{4}$$

Although the LCM frequency in the vacuum, as a initial value, should be determined, experiment by experiment, the LCM frequency measurement in the vacuum is often not easy in the atmospheric and low-pressure CVD system. Thus, the accurate measurement of the LCM frequency difference from the vacuum condition, such as $\Delta f_{\mathrm{H_2}}$ and Δf_{Mix}, is difficult.

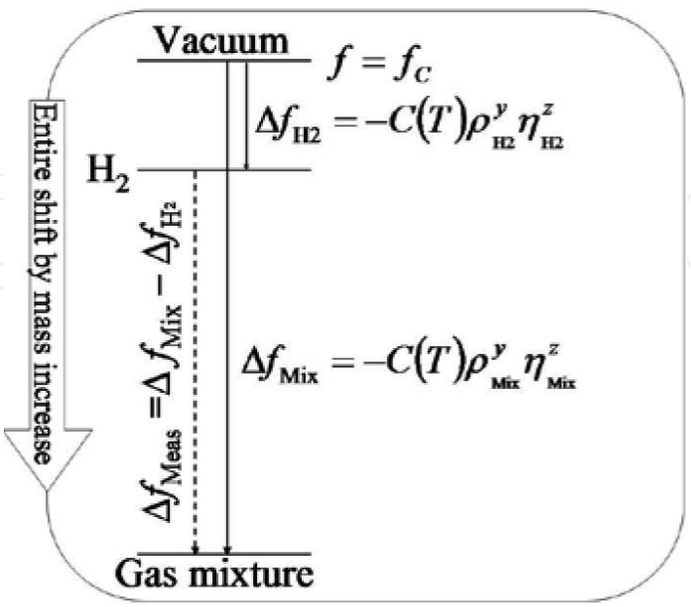

Figure 3. Frequency of langasite crystal microbalance for hydrogen and gas mixtures.

http://dx.doi.org/10.5772/62389

In contrast, the LCM frequency change at the CVD condition from the carrier gas ambient, such as hydrogen ambient, is easily measured by simple operation. The LCM frequency change from that in the hydrogen (100%), Δf_{Meas}, is expressed by Eq. (5).

$$\Delta f_{\mathrm{Meas}} = \Delta f_{\mathrm{Mix}} - \Delta f_{\mathrm{H_2}}. \tag{5}$$

Following this, the Δf_{Meas} value can be accurately determined, while the mass change of the LCM occurs by means of the multiple use of the LCM.

By evaluating the ratio of the measured LCM frequency in the gas mixture to that in hydrogen, Δf_{Meas} is shown to have a relationship with the properties as described by Eq. (6).

$$\Lambda f_{\mathrm{Meas}} = \frac{\Lambda f_{\mathrm{H_2}}}{\rho^{y}_{\mathrm{H_2}}\eta^{z}_{\mathrm{H_2}}}\rho^{y}_{\mathrm{Mix}}\eta^{z}_{\mathrm{Mix}} - \Lambda f_{\mathrm{H_2}}. \tag{6}$$

The $\Delta f_{\mathrm{H_2}}$ value can be sufficiently smaller than the first term in Eq. (6).

$$\ln \Delta f_{\mathrm{Meas}} = y \ln \rho_{\mathrm{Mix}} + z \ln \eta_{\mathrm{Mix}} + A, \tag{7}$$

where A is a constant. Using Eq. (7) accounting for various LCM frequencies and the fluid properties, the y and z values can be optimized.

In Eq. (7), the gas density and the gas viscosity are obtained following the ideal gas law and the Chapman–Enskog equation [10], respectively. The viscosity of the gas mixture is calculated following Pollard and Newman [11].

2.3. Influenced of gas density and viscosity

Figure 4 shows the Δf_{Meas} values obtained at 160, 400, 500 and 600°C using various gas mixtures, such as hydrogen–nitrogen, hydrogen–trichlorosilane, hydrogen–monomethylsilane. In this figure, the Δf_{Meas} value is plotted as a function of $\rho^{y}\mu^{z}$ assuming that both the y and z values are 0.5 following a previous study [9]. As shown in this figure, the Δf_{Meas} value follows a single trend and does not depend on the gas species. However, the behaviour shown in this figure is not linear.

Next, using Eq. (7), the y and z values are obtained. Using the measurement shown in **Figure 4**, both the y and z values are determined to be 1.3. As shown in **Figure 5**, the Δf_{Meas} value has a linear relationship with $\rho^{1.3}\mu^{1.3}$. Similar to **Figure 4**, the LCM frequency change in **Figure 5** does not depend on the gas species.

Using Eqs. (1) and (2), the $C(T)$ values at 160, 400, 500 and 600°C are obtained as shown in **Figure 6**. This figure shows that the $C(T)$ value is expressed following the Arrhenius-type behaviour.

$$C(T) = 5.4 \times 10^{11} e^{(-2100/T)} \tag{8}$$

Following Eqs. (1), (2), (5) and (8) using the y and z values of 1.3, the Δf_{Meas} value is calculated and plotted versus the measurement from 160 to 600°C, as shown in **Figure 7**. This figure shows that the calculation could sufficiently reproduce the measurement.

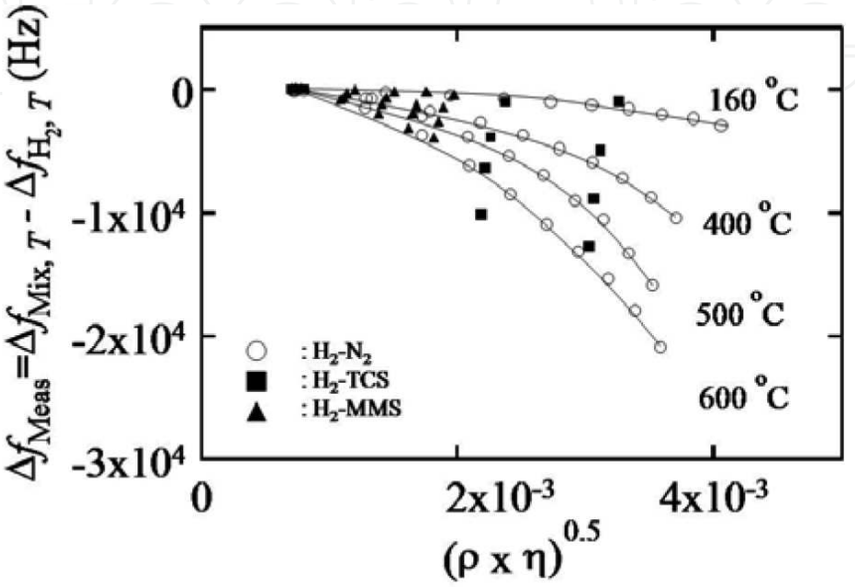

Figure 4. The Δf_{Meas} value obtained for the gas mixture containing nitrogen, trichlorosilane and monomethylsilane in the hydrogen carrier gas at 160–600°C, plotted as a function of $\rho^{0.5}\mu^{0.5}$.

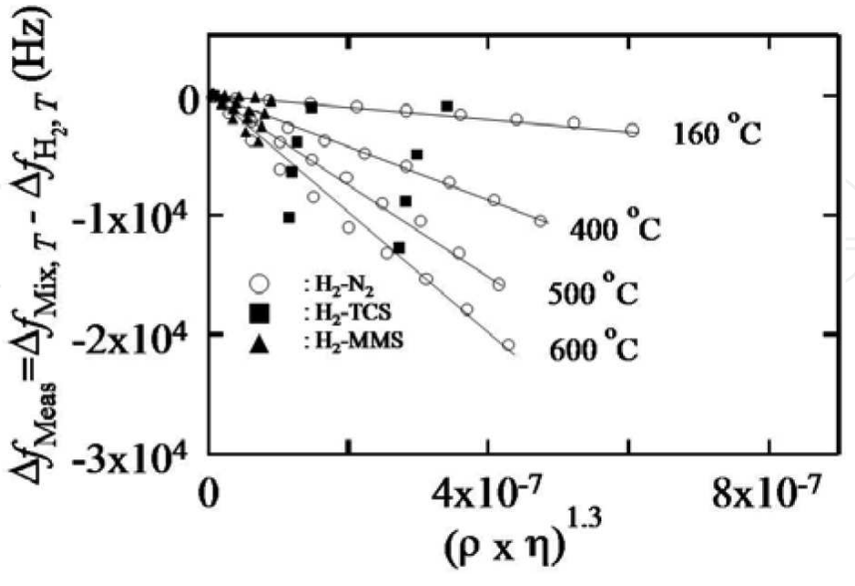

Figure 5. The Δf_{Meas} value obtained for the gas mixture containing nitrogen, trichlorosilane and monomethylsilane in the hydrogen carrier gas at 160–600°C, plotted as a function of $\rho^{1.3}\mu^{1.3}$.

http://dx.doi.org/10.5772/62389

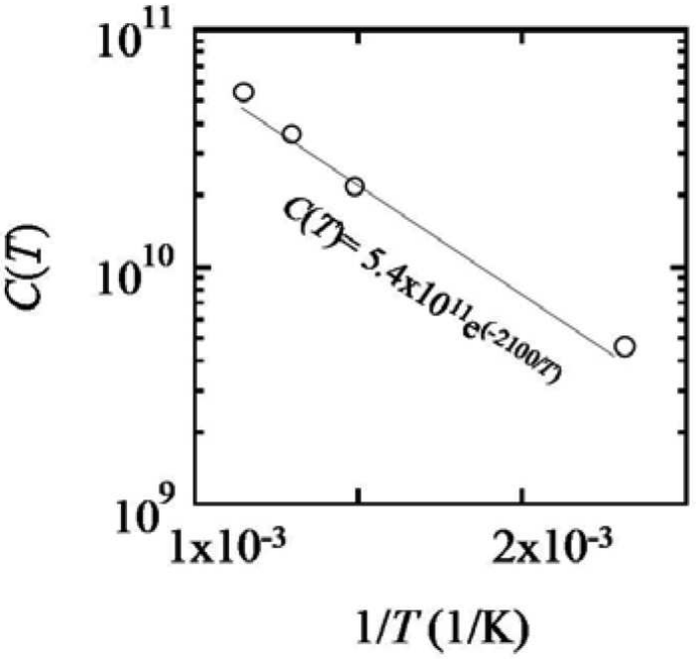

Figure 6. $C(T)$ values changing with $1/T$.

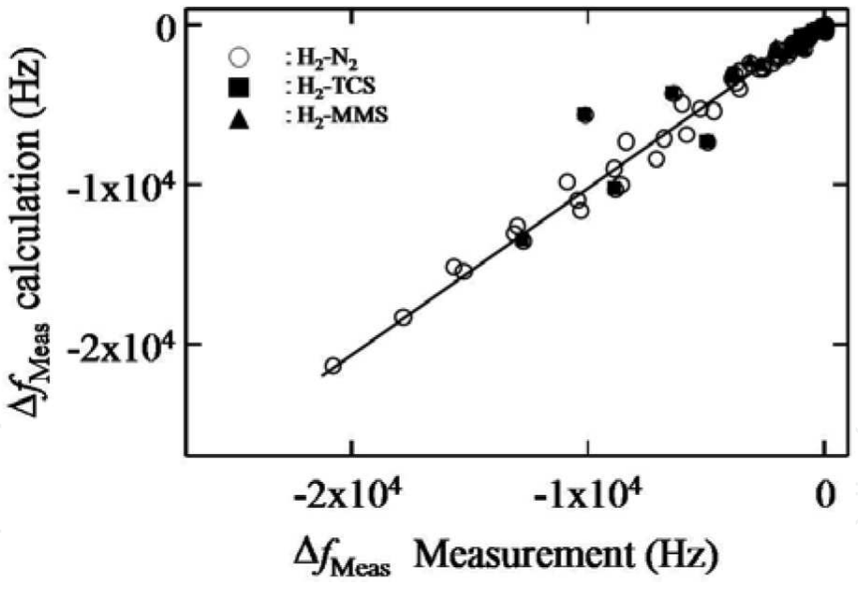

Figure 7. Correlation of the Δf_{Meas} values between the measurement and the calculation by Eqs. (1), (2), (5) and (8) using y and z of 1.3 at the temperatures of 160–600°C.

3. Method for determining chemical vapour deposition occurrence

In this section, the method for determining the surface chemical reaction occurrence [12] is explained. The silicon carbide film formation from monomethylsilane gas is discussed.

3.1. LCM frequency

The LCM frequency differences from ambient hydrogen in monomethylsilane–hydrogen system are shown in **Figure 8**. Immediately after opening the gas valve at 0 s, a high concentration of monomethylsilane gas, remained at 100% between the gas valve and the mass flow controller, is introduced into the reactor. During the high concentration gas passing through the reactor, the LCM frequency significantly decreases. Thereafter, the diluted monomethylsilane gas reaches the LCM in the reactor. Thus, the fluctuation of the LCM frequency becomes quite small.

As shown in **Figure 8**, the LCM frequency difference measured at 300°C is very stable after 20 s. This indicates that the gas temperature and the fluid properties, such as the gas density and gas viscosity, are in a steady state. This simultaneously indicates that there is no chemical reaction at 300°C, due to no thermal change caused by no reaction heat. The behaviour at 400 and 500°C is similar to that at 300°C. The trend in the LCM frequency difference at 300, 400 and 500°C is the same and parallel to each other. Thus, the MMS-H_2 system below 500°C is concluded to undergo no chemical reaction.

Although the LCM frequency difference at 550°C seems to be relatively stable, it very gradually increases after 20 s. Similar to this, the LCM frequency difference at 600°C also slightly increases with a larger gradient than that at 550°C. This gradual increase in the LCM frequency difference indicates that any transient change related to a chemical reaction, such as temperature, gas density and gas viscosity, occurred and continued in the reactor during the introduction of the monomethylsilane gas.

As shown in **Figure 8**, the LCM frequency increases with the decreasing temperature [13]. Additionally, the surface chemical reaction for the silicon carbide (SiC) film deposition from the monomethylsilane gas is endothermic [13]. The frequency decrease due to the weight

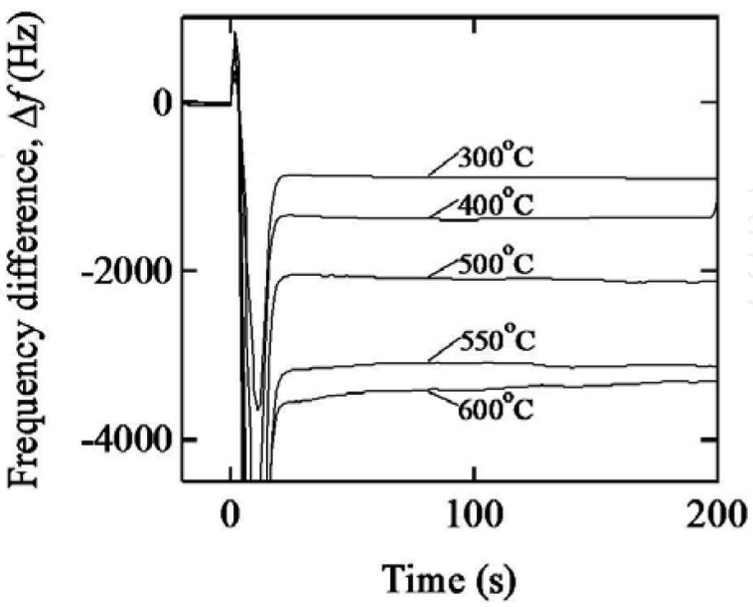

Figure 8. The LCM frequency change immediately after the introduction of the monomethylsilane gas to the hydrogen ambient atmosphere.

http://dx.doi.org/10.5772/62389

increase by the film deposition is overcompensated by the frequency increase due to the temperature decrease by the endothermic reaction. Thus, the LCM frequency continues to increase till reaching a steady state. From **Figure 8**, the chemical reaction occurring at the LCM surface is considered to continue after 200 s.

The temperature change should be enhanced by the increasing reaction rate, due to the greater reaction heat. In order to clearly show this trend, the LCM frequency gradient at various temperatures for the monomethylsilane–hydrogen system is evaluated, as shown in **Figure 9**. The LCM frequency gradient in the low-temperature range between 300–500°C is <0 Hz/s. This value is recognized to show the state with no chemical reaction. In contrast, the LCM frequency gradient increases at 550°C from a value <0 to the positive value of 2 Hz/s. It further increases to a value >4 Hz/s at 600°C. Because the LCM frequency gradient increases with the increasing temperature, the surface chemical reaction at the LCM surface is initiated in the temperature range between 500 and 600°C.

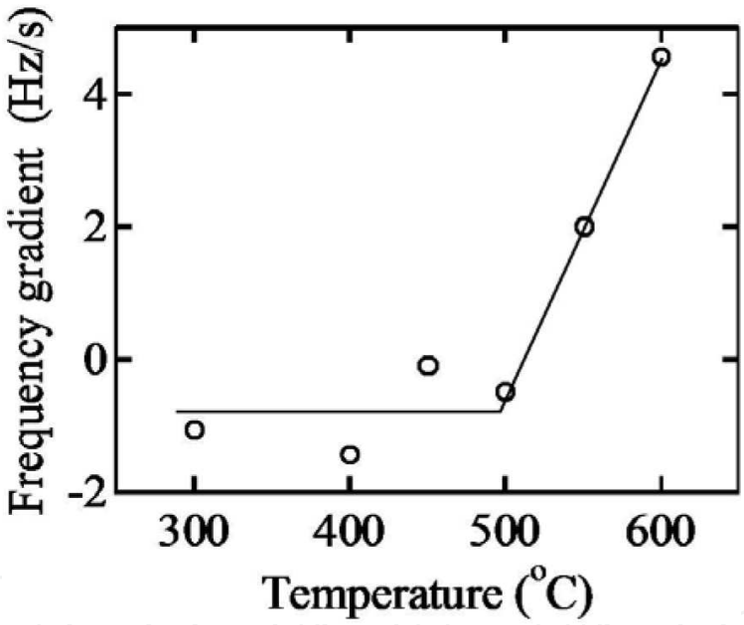

Figure 9. LCM frequency gradient immediately after introducing the MMS gas at various temperatures.

3.2. *C*(*T*) parameter

Figure 10 shows the LCM frequency change with the increase in $\rho_{Mix}^{1.3}\eta_{Mix}^{1.3}$ of the gas mixtures of monomethylsilane, nitrogen and hydrogen at 400, 500 and 600°C. In this figure, the frequency difference of the nitrogen–hydrogen system (white circles) follows Eq. (1) (x and y = 1.3) and shows a linear relationship. The monomethylsilane–hydrogen system (triangles) at 400 and 500°C coincides with the behaviour of the nitrogen–hydrogen system. In contrast, the monomethylsilane–hydrogen system showed a slightly higher gradient in the low $\rho^{1.3}\eta^{1.3}$range. Thus, the $C(T)$ value of Eq. (1) is expected to indicate the occurrence of a surface chemical reaction.

The $C(T)$ values obtained using Eq. (1) are plotted versus $1/T$. as shown in **Figure 11**. The $C(T)$ values for the nitrogen–hydrogen system have a linear relationship following Arrhenius-type equation at temperatures from 300 to 600°C. In contrast, the monomethylsilane–hydrogen system shows an increase in the $C(T)$ value at the higher temperatures.

In order to clearly recognize the difference, the $C(T)$ value difference of the monomethylsilane–hydrogen system from the nitrogen–hydrogen system are shown in **Figure 12**. The $C(T)$ value difference at temperatures lower than 500°C is around zero. Thus, the monomethylsilane gas at <500°C behaves the same as that of nitrogen. The monomethylsilane–hydrogen system shows an increased $C(T)$ value to $>1 \times 10^{10}$ at temperatures between 500 and 550°C. Because these values are obtained separate from the fluid properties, the $C(T)$ value change is understood as the surface chemical reaction for the CVD occurring at the higher temperatures. The obtained temperature is consistent with that from our previous study [6].

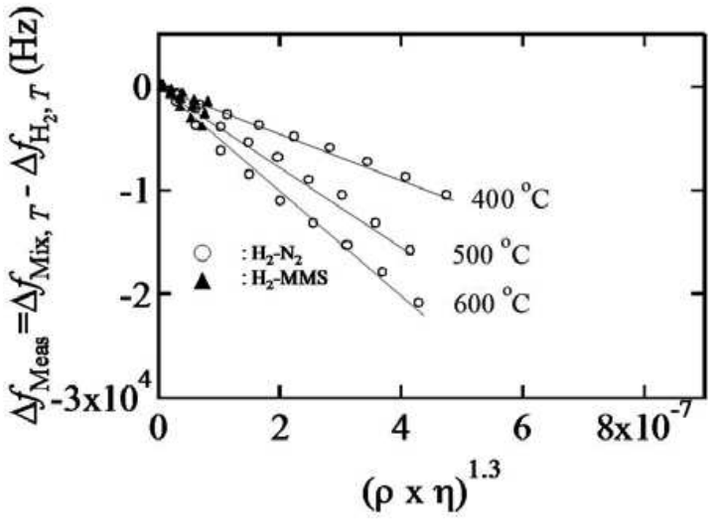

Figure 10. LCM frequency difference for monomethylsilane gas (dark triangle) and nitrogen gas (circle) from ambient hydrogen.

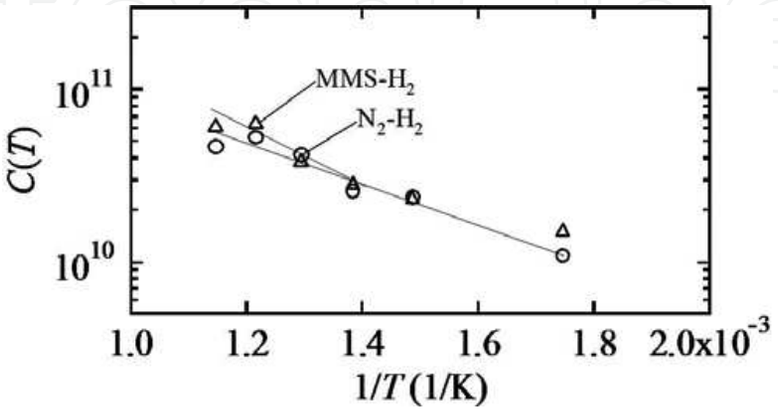

Figure 11. $C(T)$ values of monomethylsilane–hydrogen system (triangles) and nitrogen–hydrogen system (circles).

http://dx.doi.org/10.5772/62389

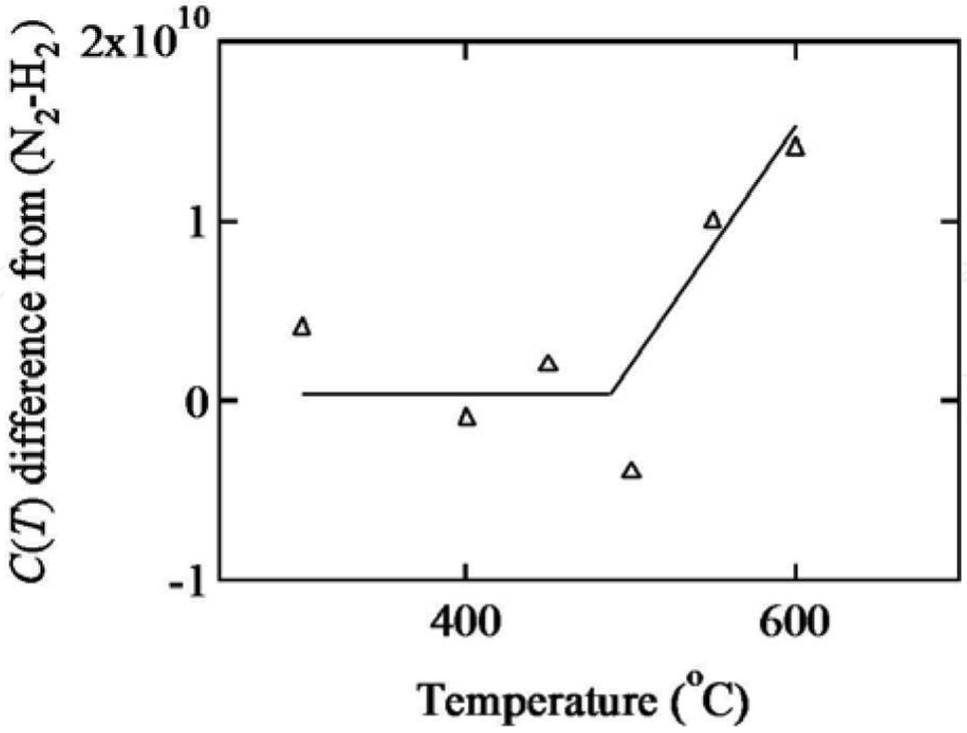

Figure 12. $C(T)$ value difference of MMS–H_2 system from N_2–H_2 system.

4. *In situ* observation of chemical vapour deposition using $SiHCl_3$ and BCl_3 gases

The film deposition behaviour using multiple precursors is explained [14]. The boron-doped silicon film is formed using the trichlorosilane ($SiHCl_3$, TCS) gas and the boron trichloride (BCl_3) gas for the film deposition and boron doping, respectively.

4.1. Chemical reaction occurrence

The chemical reaction behaviour of boron trichloride gas is measured, as shown in **Figure 13**, at various boron trichloride concentrations and temperatures. At 400°C, the LCM frequency quickly decreases corresponding to the change in the fluid properties by an increase in the boron trichloride concentration. The LCM frequency is kept constant at each boron trichloride concentration. Thus, the boron trichloride gas does not have any chemical reaction and film deposition at this temperature. At 470°C, the LCM frequency sometimes shows flat and other times decrease. The film deposition occurrence is not obvious. In contrast, at 570°C, the LCM frequency decrease is clear at each boron trichloride concentration, as the typical behaviour showing the film deposition.

Similarly, the silicon film deposition from trichlorosilane gas is evaluated. Because the LCM frequency decrease occurs between 570 and 600°C, the silicon film deposition is determined to occur in this temperature range.

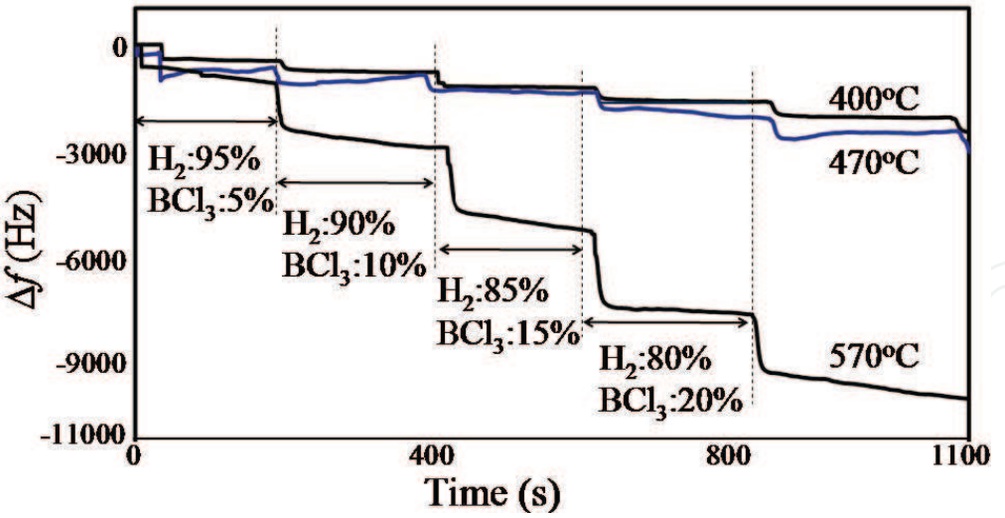

Figure 13. LCM frequency change at various boron trichloride concentrations and at 400, 470 and 570°C.

Next, the LCM frequency behaviour during the boron-doped silicon film deposition is observed at various temperatures using the trichlorosilane and boron trichloride gases, as shown in **Figure 14**. The LCM frequency shows a gradual increase and decrease in a short cycle at 330–500°C. In contrast, at 530 and 570°C, the LCM frequency continuously decreases.

Figure 15 shows the LCM frequency gradient in the temperature range between 330 and 570°C. At temperatures lower than 470°C, the frequency gradient values are near 0 Hz s^{-1}. At the temperatures higher than 500°C, the frequency gradient decreases to less than −3 Hz s^{-1}. This behaviour indicates the occurrence of a continuous film deposition. Because the LCM frequency decreases for a long period, the film deposition is determined to occur in the temperature range between 470 and 530°C, specifically higher than 530°C.

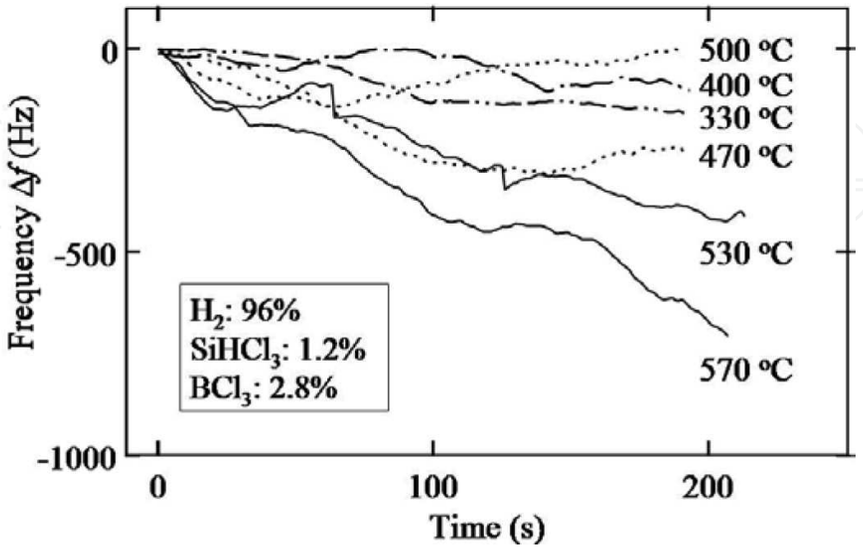

Figure 14. LCM frequency change at various trichlorosilane and boron trichloride concentrations at 330–570°C.

http://dx.doi.org/10.5772/62389

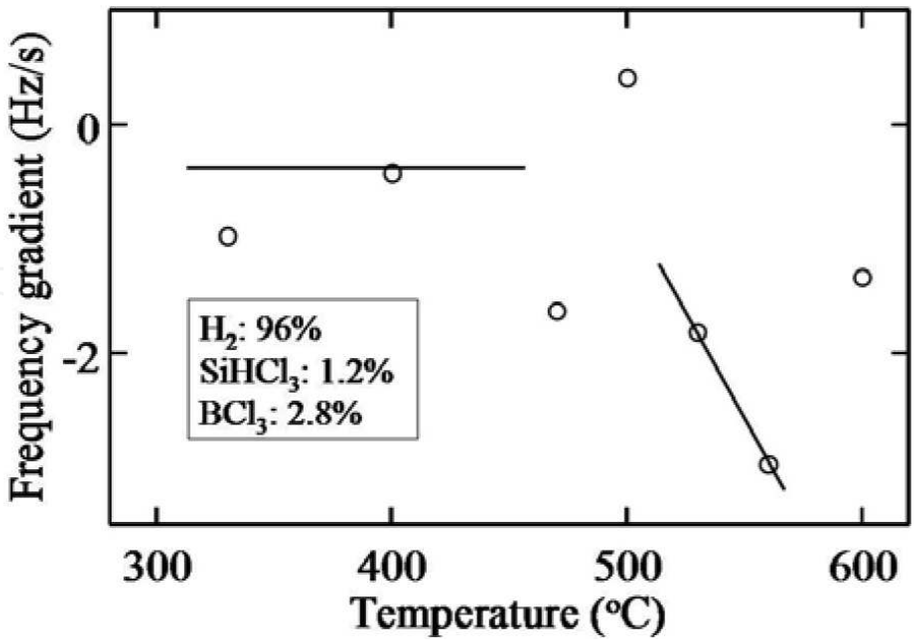

Figure 15. LCM frequency gradient in the temperature range between 330 and 570°C. The trichlorosilane and boron trichloride gases were used for the film formation.

4.2. Growth rate

The film growth rate is shown in **Figure 16**, obtained following that the frequency decrease of 1 Hz corresponds to the weight increase of 6 ng cm^{-2} [9, 13, 15]. Here, the molecular weight and the density of the boron-doped silicon film are tentatively assumed to be an average of the silicon and boron.

The boron film growth rate at 570°C is near 1.5×10^{-9} mol cm^{-2} s^{-1} at the boron trichloride gas concentrations from 1 to 4%. Additionally, the silicon growth rate shows no obvious trend versus the trichlorosilane gas concentration from 1 to 4%. Similarly, the growth rate of the boron-doped silicon film formed from both the trichlorosilane and boron trichloride gases has no obvious trend, being about 1×10^{-9} mol cm^{-2} s^{-1}. This growth rate behaviour is consistent with the saturation in the low-temperature silicon epitaxial growth process [16].

The change in the growth rate with the increasing temperature is shown in **Figure 17** as the Arrhenius plot. The boron growth rate is near 1×10^{-9} mol cm^{-2} s^{-1} and 1.5×10^{-9} mol cm^{-2} s^{-1} at 470 and 570°C, respectively. The silicon growth rate from trichlorosilane gas is about 5×10^{-10} mol cm^{-2} s^{-1} at temperatures lower than 530°C. It is too low value for determining the film deposition occurrence. Because the growth rate increases to nearly 10^{-9} mol cm^{-2} s^{-1} at 600°C, the silicon film deposition occurs at temperatures higher than 570°C.

At temperatures lower than 530°C, the film growth rate is about 5×10^{-10} mol cm^{-2} s^{-1}. Because this value is similar to that of silicon, the film deposition is negligible. In contrast, the growth rate increases at temperatures higher than 530°C. It reaches 1×10^{-9} mol cm^{-2} s^{-1} at 570°C. The boron-doped silicon film is expected to be obtained at 570°C.

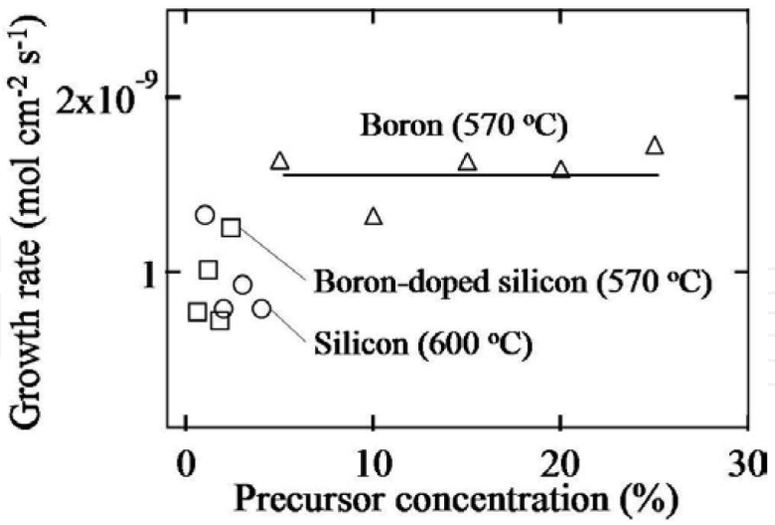

Figure 16. Growth rate at various trichlorosilane and boron trichloride gas concentrations. Silicon and boron film was grown using the combinations of trichlorosilane and boron trichloride gases of 2.4 and 1.0, 1.8 and 1.8, 1.2 and 2.8, and 0.6 and 4.0%.

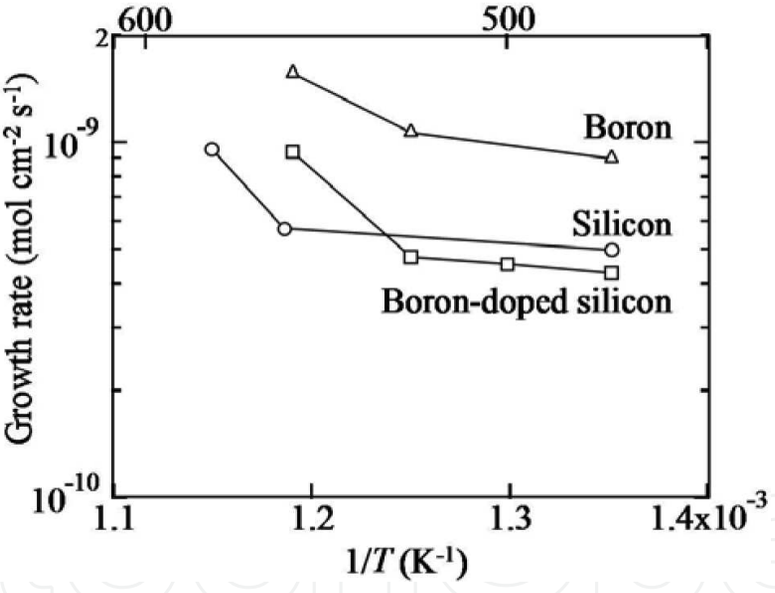

Figure 17. Film growth rates changes of silicon, boron and boron-doped silicon versus 1/*T*.

4.3. Film formation on substrate

The boron-doped silicon film is formed at 570°C using the trichlorosilane gas and boron trichloride gas at 5 and 3%, respectively. The depth profile of the boron concentration is evaluated by secondary ion mass spectrometry (SIMS), as shown in **Figure 18**. While the boron concentration in the substrate is about 5×10^{16} atoms cm^{-3}, it increases to that higher than 10^{20} atoms cm^{-3} near the film surface. Because the obtained film thickness is about 100 nm, the film growth rate is about 6–7 nm min^{-1}. This value is comparable to 4 nm min^{-1} estimated from

http://dx.doi.org/10.5772/62389

Figures 16 and **17**. Thus, the growth rate obtained by the LCM is consistent with that by the film growth on the substrate.

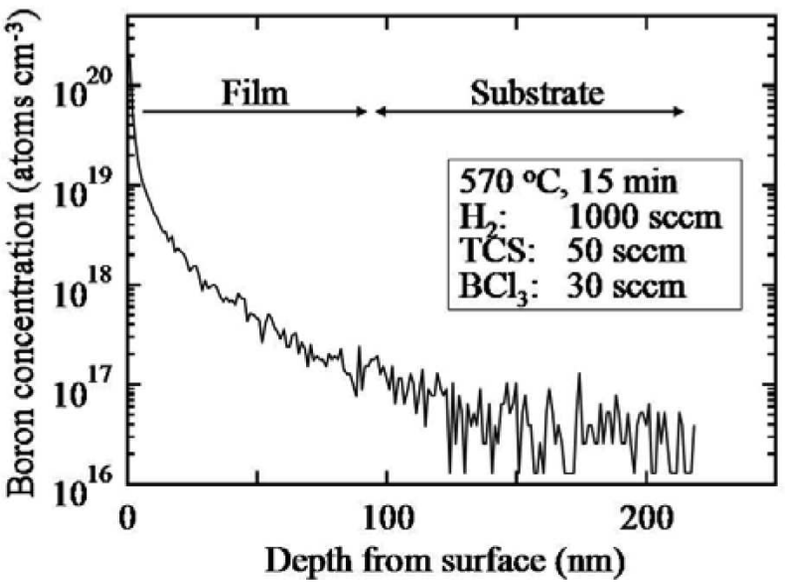

Figure 18. Depth profile of boron concentration in the obtained silicon film.

4.4. Surface process

The behaviours of film growth and doping are explained using Eqs. (9)–(12). The symbol '*' indicates the chemisorbed state. Trichlorosilane is chemisorbed at the surface to produce $*SiCl_2$ and hydrogen chloride gas; $*SiCl_2$ is decomposed by hydrogen to form silicon at the surface [15]. Similarly, $*BCl_2$ is considered to be formed at the surface; it reacts with hydrogen to produce boron.

$$SiHCl_3 \rightarrow *SiCl_2 + HCl\uparrow \tag{9}$$

$$*SiCl_2 + H_2 \rightarrow Si + 2HCl\uparrow \tag{10}$$

$$BCl_3 + \frac{1}{2}H_2 \rightarrow *BCl_2 + HCl\uparrow \tag{11}$$

$$*BCl_2 + H_2 \rightarrow B + 2HCl\uparrow \tag{12}$$

For both gases, the intermediate species are chlorides which terminate the surface. The film growth rate at low temperatures is governed by the rates of the intermediate species adsorption and the chlorine removal. Thus, the growth rate of the boron-doped silicon is influenced by

the slower process, that is by the silicon film growth rate. Because the LCM detects such details of the various behaviours, it can work as a sensitive monitor for studying the film growth behaviour.

5. Temperature change related to film formation process

The surface temperature is one of the most important parameters for the CVD. In this section, the LCM is used in order to reveal and clarify the temperature behaviour related to the film formation [17]. For this purpose, the silicon film formation in a trichlorosilane–hydrogen system is used as one of the most popular systems.

5.1. LCM frequency behaviour

The LCM frequency decreases corresponding to the weight increase on the LCM surface, following the Sauerbrey equation [15].

$$\Lambda f = -\frac{\Delta m f_0^2}{A\left(\mu_c \rho_c\right)^{0.5}}, \tag{13}$$

where Λf is the measured resonant frequency decrease, f_0 is the intrinsic crystal frequency, Δm is the elastic mass change, A is the electrode area, ρ_c is the density of the crystal, and μ_c is the shear modulus of the crystal.

Additionally, the LCM frequency depends on the fluid properties, as described by equation (14) [7, 8, 18].

$$\Lambda f \propto \left(\rho\eta\right)^x, \tag{14}$$

where ρ and η are the density and the viscosity, respectively, of the gas mixture. The η value is obtained from the literature [11]. The x value is 1.3 [7] in this section.

These parameters produce various changes in the LCM frequency during the CVD process. The change in the LCM frequency related to the film deposition by the trichlorosilane gas is classified by Parameters (*i*)–(*viii*) schematically shown in **Figure 19**.

Parameter (*i*) in **Figure 19** is the pressure and concentration of the gas remaining in the gas system. The LCM frequency very quickly and slightly increases due to the pressure increase in the reactor when opening the trichlorosilane gas valve. Immediately after this, the LCM frequency decreases and soon recovers by the trichlorosilane gas, which is remained at a high concentration in the gas line, reaching and passing the reactor. Parameter (*ii*) is the $(\rho\eta)^{1.3}$ value of the gas mixture. Corresponding to this, the LCM frequency decreases from the initial frequency. Parameter (*iii*) is the heat capacity and the heat conduction. The increase in the heat

http://dx.doi.org/10.5772/62389

capacity gradually causes the gas-phase temperature to decrease, resulting in an increase in the LCM frequency. Parameter (*iv*) is the reaction heat. The silicon film formation is an endothermic reaction [19]. This decreases the temperature and thus increases the LCM frequency. With the addition of the trichlorosilane gas, the film formation quickly begins and continues till termination of the trichlorosilane gas supply. Parameter (*v*) is the weight increase due to the film deposition. After a sufficient time for reaching a steady state, the weight increase by the film formation on the LCM appears as a continuous and linear decrease in the LCM frequency. Parameter (*vi*) is the $(\rho\eta)^{1.3}$ value. The decrease in this value immediately causes the LCM frequency to shift to a high value when the trichlorosilane gas supply is terminated. Parameter (*vii*) is the heat capacity and the heat conduction. Due to the heat capacity decrease because of the lack of trichlorosilane gas, the gas-phase temperature gradually increases and causes a decrease in the LCM frequency. Parameter (*viii*) is the weight increase due to the film deposition. After a sufficient period for achieving a steady state, the LCM frequency shift from that before the trichlorosilane gas supply corresponds to the increased weight of the film formed on the LCM.

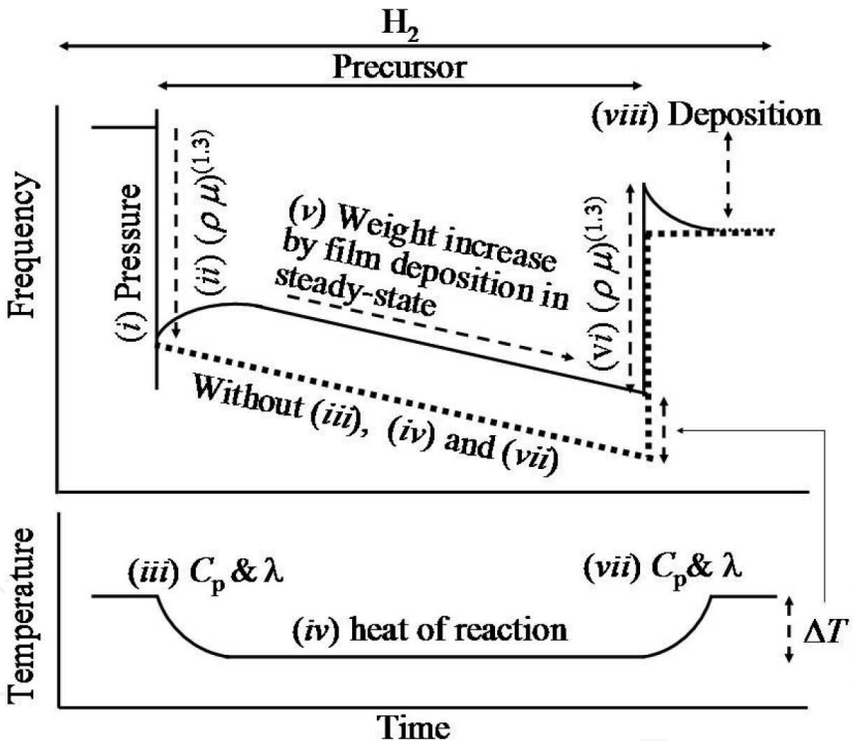

Figure 19. Schematic of changes in the frequency and the temperature of the LCM influenced by various parameters. Parameter (*i*): pressure and concentration of gas remaining in the gas system, parameter (*ii*): $(\rho\eta)^{1.3}$, parameter (*iii*): heat capacity, parameter (*iv*): reaction heat, parameter (*v*): weight increase due to the film deposition, parameter (*vi*): $(\rho\eta)^{1.3}$, parameter (*vii*): heat capacity and parameter (*viii*): weight increase due to the film deposition.

If the temperature change due to the trichlorosilane gas did not exist, the temperature during the early stage of the film formation behaves like the thick dotted line, as shown in **Figure 19**. Thus, the LCM frequency difference between the solid line and the thick dotted line is considered to be a function of the temperature shift.

5.2. Reaction heat and heat transport

By introducing the trichlorosilane gas into the reactor, the silicon film formation occurs along with the endothermic reaction heat and change of the physical properties of the gas mixture, as shown in **Figure 20**. Thus, the multiple thermal processes change the surface temperature. Here, the influence of each parameter is evaluated, following Steps 1, 2 and 3, as shown in **Figure 21**, taking into account the time constant for heat transport.

During Step1, the time constant for the surface temperature shift is evaluated without introducing a precursor in the ambient hydrogen. The quick lamp power decrease is assumed to show a significantly quick surface temperature decrease similar to that by the endothermic surface chemical reaction, as shown in **Figure 20**. After this, the gas-phase temperature of the near-surface region gradually decreases. These two processes are expected to have different time constants, such as very short and slightly long.

During Step 2, the influence of the change in the heat capacity and the heat conduction of the gas mixture are explained. The time constant for the gas-phase temperature shift induced by the precursor introduction, as shown in **Figure 20**, is evaluated at sufficiently low temperatures at which no chemical reaction occurs. The time constant for this process is expected to be longer than those for Step 1, because the gas-phase temperature shift occurs in the entire region of the reactor and not limited to the region near the surface.

During Step 3, the temperature change related to the film deposition is explained, accounting for the time constants obtained in Steps 1 and 2. During Step 3, the trichlorosilane concentration is stepwise changed from 0 to 3%. After the period corresponding to the time constants obtained in Steps 1 and 2, the LCM frequency behaviour expresses the film formation in a steady state. By extrapolation, the LCM frequency immediately after changing the precursor concentration is used for evaluating the temperature shift related to the film formation.

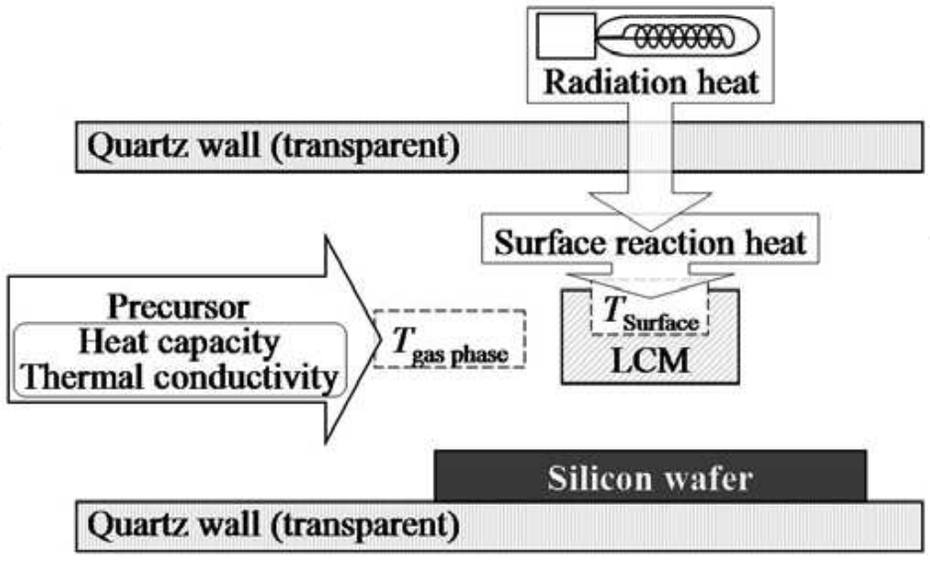

Figure 20. Parameters influencing the LCM temperature.

http://dx.doi.org/10.5772/62389

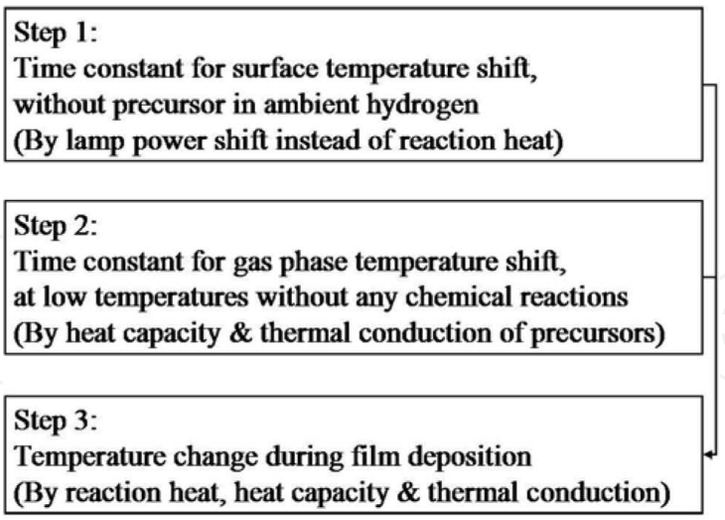

Figure 21. Three steps for evaluating temperature change during film deposition

5.3. Temperature and frequency

The entire frequency dependence on the temperature is shown in **Figure 22**. This shows the frequency difference at various temperatures from that at room temperature. With the increasing temperature, the LCM frequency decreases, as shown in **Figure 22a**. At the higher temperatures, the LCM frequency more rapidly decreases than that at the lower temperatures. The temperature gradient is shown in **Figure 22b**. The gradient decreases with the increasing temperature. The frequency change due to the temperature change is about −400 Hz/K in the temperature range between 500 and 650°C.

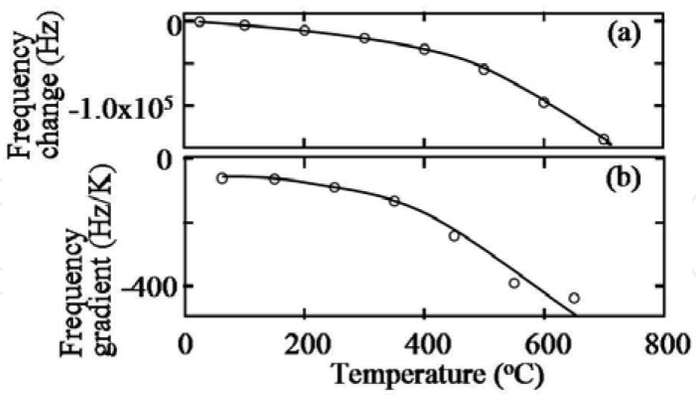

Figure 22. LCM frequency changing with the temperature. (a) frequency change from that at room temperature and (b) frequency gradient (Hz/K) at various temperatures.

5.4. Heat at surface

In order to evaluate the LCM frequency behaviour caused by the quick surface temperature decrease, such as that by the reaction heat, the LCM frequency influenced by the stepwise lamp

power shift is evaluated, as shown in **Figure 23**. The lamp power corresponding to about 1 K quickly decreases at 450 and 660°C.

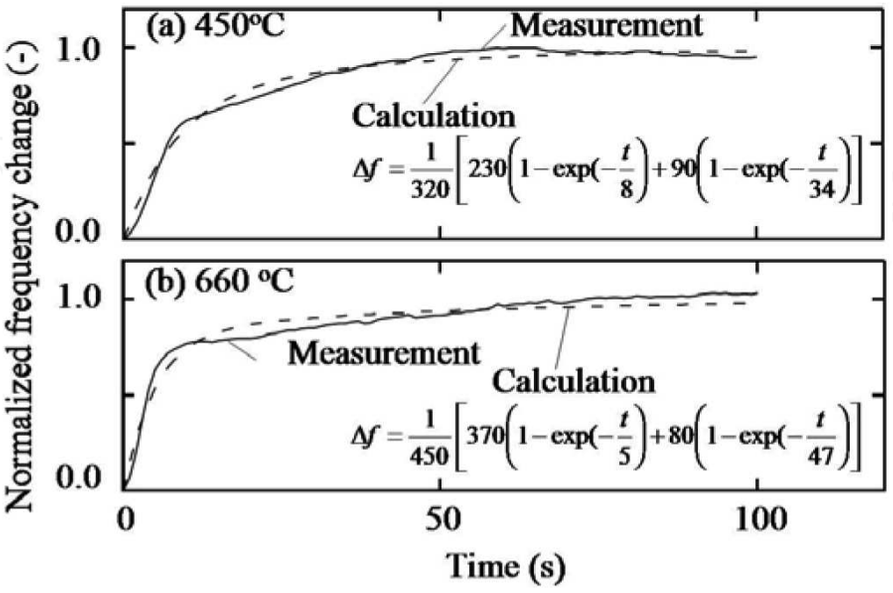

Figure 23. LCM frequency change caused by the stepwise lamp power shift corresponding to about 1 K at (a) 450°C and (b) 660°C.

Figure 23a and **23b** shows the normalized LCM frequency change caused by the stepwise lamp power shift at 450 and 660°C, respectively. In both figures, the LCM frequency very quickly increases immediately after changing the lamp power. It then moderately increases and reaches the steady state.

These behaviours are expressed as a function of time, t (s), assuming that the fast and slow relaxation processes.

$$\Delta f = \left[230\left(1-e^{\left(-\frac{t}{8}\right)}\right)+90\left(1-e^{\left(-\frac{t}{34}\right)}\right)\right]. \tag{15}$$

$$\Delta f = \left[370\left(1-e^{\left(-\frac{t}{5}\right)}\right)+80\left(1-e^{\left(-\frac{t}{47}\right)}\right)\right]. \tag{16}$$

In **Figure 23**, Eqs. (15) and (16) are indicated by the dotted lines. The quick temperature change, the first term, is considered to directly follow the lamp power decrease, that is the decrease in heat at the LCM surface. The slow temperature change, the second term, is due to the conduction heat transport between the surface and the gas phase very near the surface. The influence of the reaction heat and heat conduction on the LCM frequency is expected to appear within 10 and 50 s, respectively, after introducing the trichlorosilane gas.

http://dx.doi.org/10.5772/62389

5.5. Heat transport around surface in gas phase

The LCM frequency changes due to the thermal properties, such as the heat capacity and the heat conductivity, are evaluated at the low temperatures, which do not cause the film deposition [14]. **Figure 24** shows that the LCM frequency change is due to the stepwise concentration change of hydrogen gas and trichlorosilane gas at 380°C. At conditions C_A–C_E, the hydrogen concentration and the trichlorosilane concentration decrease and increase, respectively.

At the beginning of condition C_A, the LCM frequency quickly drops to less than −3000 Hz and recovers to −1000 Hz. The LCM frequency shift from 0 Hz to −1000 Hz corresponds to the increase in the gas density and the gas viscosity. Next, it gradually recovers to near −400 Hz. Till 500 s, the LCM frequency reaches the steady state. The gradual recovery of the LCM frequency is a result of the temperature decrease mainly due to the increase in the heat capacity of the gas mixture. Additionally, the temperature decrease at the surface is moderated by the heat balance with the gas phase *via* the heat conduction.

These heat transports overlaps and gives the gradual recovery of the LCM frequency. The LCM frequency at 380°C and at condition C_D is expressed, as shown in **Figure 25**, using the following equation.

$$\Delta f = 164\left(1 - e^{\left(-\frac{t}{120}\right)}\right). \tag{17}$$

From the temperature shift width shown in **Figure 25**, the temperature decrease by the trichlorosilane gas concentration change at 380°C is about 1 K. The time constant of these process is about 120 s. The time constant in Eq. (17) is longer than that of the second term in Eqs. (15) and (16). The time constant is assumed to have a similar value at the higher temperatures, such as 600–700°C.

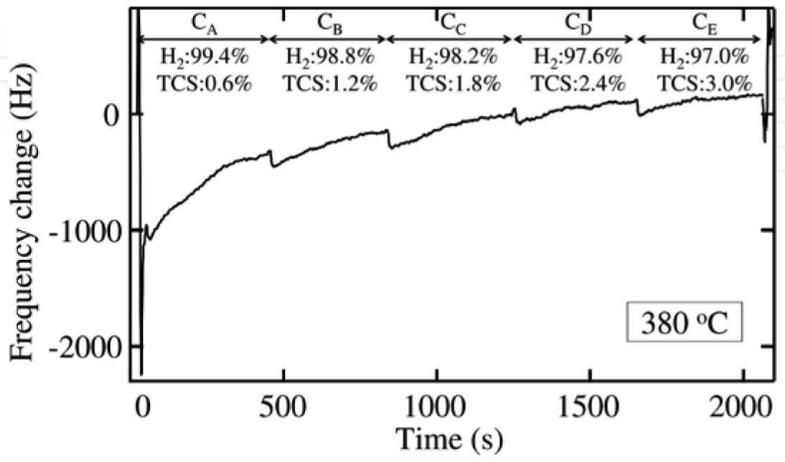

Figure 24. LCM frequency change caused by the stepwise concentration change in the hydrogen gas and trichlorosilane gas at 380°C.

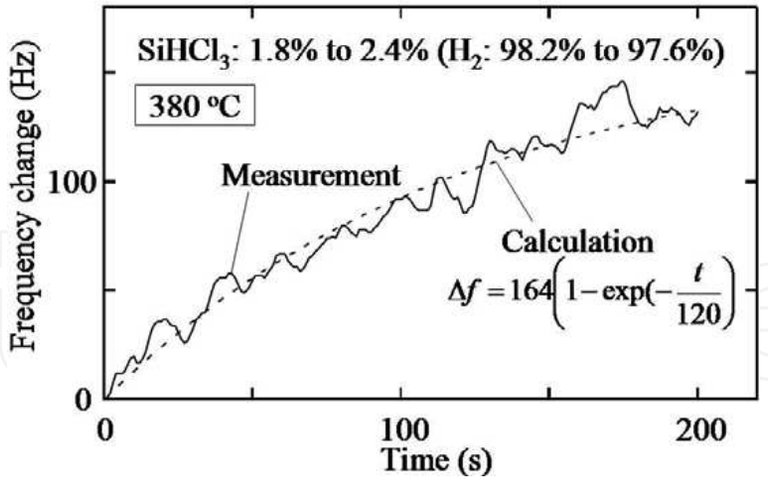

Figure 25. LCM frequency change at 380°C caused by the gas concentrations of hydrogen and trichlorosilane from condition C_C to C_D in **Figure 24**.

5.6. Film formation

The silicon film is formed at 640°C along with measuring the LCM frequency, as shown in **Figures 26** and **27**. The hydrogen gas concentration decreases from 100 to 97%, while the trichlorosilane gas concentration increases from 0 to 3%. Because the silicon film growth rate is saturated at this temperature [16], the reaction heat remains the same for conditions C_A–C_E.

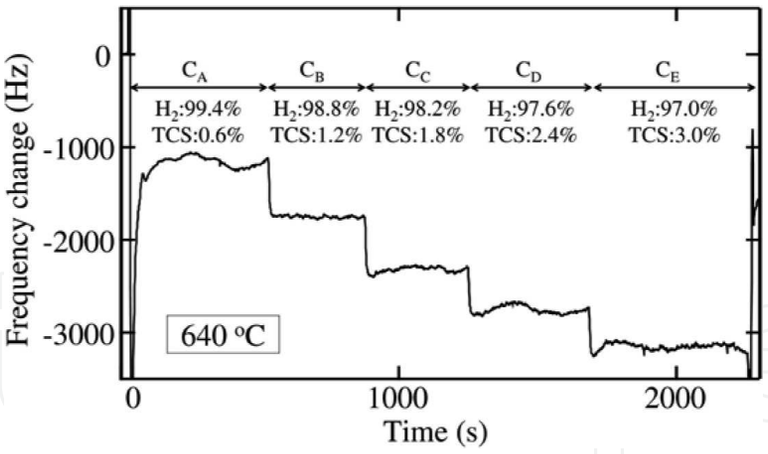

Figure 26. LCM frequency change caused by the stepwise change in the concentrations of hydrogen and trichlorosilane.

At condition C_A, the trichlorosilane gas is added to the hydrogen gas. The LCM frequency shows a significant drop and a quick recovery within several seconds. After the quick recovery, the LCM frequency gradually increases. After the peak appearance, the LCM frequency gradually decreases accompanying the fluctuation due to a temperature fluctuation. Conditions C_C, C_D and C_E show a similar LCM frequency behaviour without a significant drop, unlike that at the beginning of condition C_A.

http://dx.doi.org/10.5772/62389

Taking into account the time constant corresponding to the various heat processes, the LCM frequency behaviour is evaluated, as shown in **Figure 27**. This shows the LCM behaviour at condition C_D, as an example. Immediately after increasing the trichlorosilane concentration from 1.8 to 2.4%, the LCM frequency quickly decreases to about −550 Hz due to the increase in the gas density and the gas viscosity. Next, it shows a broad bottom for about 20 s. The LCM frequency gradually increases from 50 to 180 s. After showing a peak, the LCM frequency begins to decrease. This decrease is due to the film formation during the steady state.

Next, the LCM frequency gradient is evaluated. The maximum and minimum values are 1.6 Hz/s between Points A and B and 0.77 Hz/s between Points A and C, respectively. By this operation, the LCM frequency immediately after changing the trichlorosilane concentration is 245 to 410 Hz, as shown in **Figure 27**.

In addition, the flat bottom of the LCM frequency to 20 s after changing the trichlorosilane concentration may be caused by the balance among the changes in the gas density, the gas viscosity, the heat capacity and the heat conductivity. In order to obtain the possible minimum frequency value, the increasing trend in the LCM frequency between 20 and 180 s is extrapolated to that near several seconds. By this estimation, the frequency of about 50 Hz may be lower than that at the bottom. By adding these values, the LCM frequency change due to the temperature change by changing the trichlorosilane concentration from 1.8 to 2.4% is between 295 and 460 Hz. The surface temperature shift caused by changing the precursor concentration is considered to be about one degree.

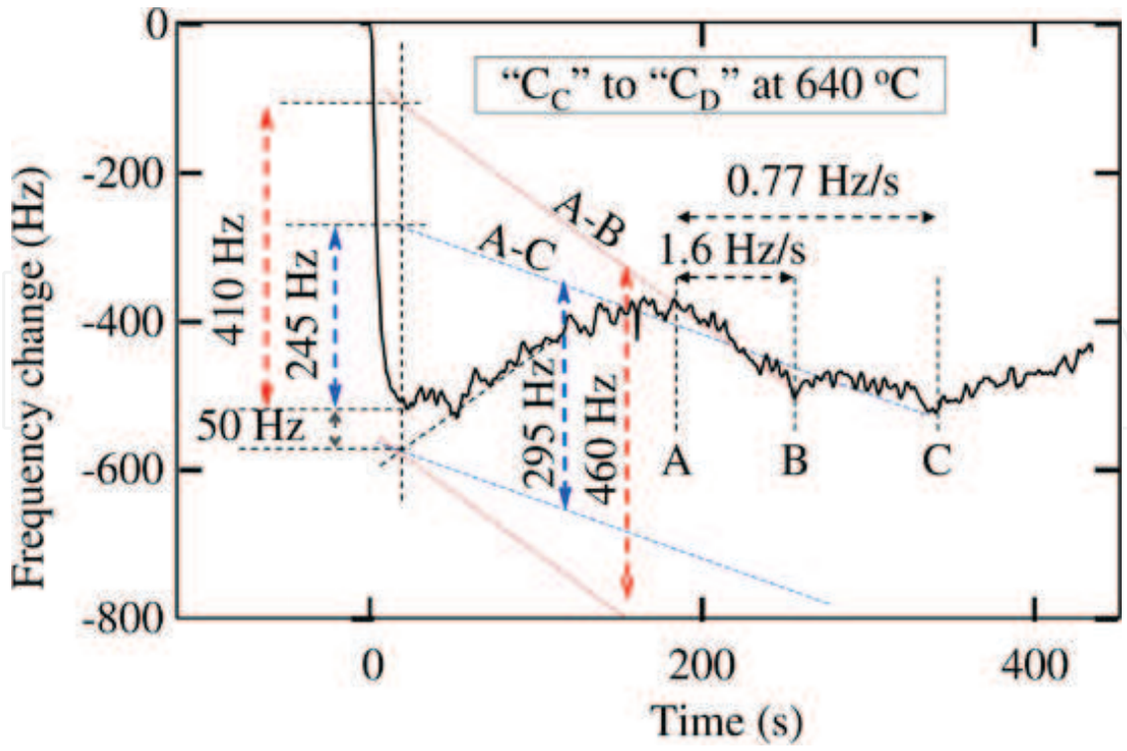

Figure 27. Evaluation of frequency change caused by the stepwise change from condition C_C to C_D in **Figure 26**.

Acknowledgements

The author would like to thank Ms. Misako Matsui, Ms. Ayumi Saito and Mr. Kento Miyazaki of Yokohama National University for their intensive work. The author would like to thank Mr. Nobuyoshi Enomoto and Mr. Hitoshi Ueno of Halloran Electronics Co., Ltd., for his technical support. A part of this study was supported by JSPS KAKENHI Grant No. 25420772.

Author details

Hitoshi Habuka*

Address all correspondence to: habuka1@ynu.ac.jp

Department of Chemical Energy Engineering, Yokohama National University, Yokohama, Japan

References

[1] S. M. Sze, Semiconductor devices: physics and technology (John-Wiley, Hoboken, NJ, 2008).

[2] A. Bouteville, "Numerical simulation applied to chemical vapor deposition process, rapid thermal CVD and spray CVD", J. Optoelectron. Adv. Mater., 7 (2005) 599–606.

[3] U. Koehler, L. Andersohn and B. Dahlheimeer, "Time-resolved observation of CVD-growth of silicon on Si (111) with STM", Appl. Phys. A, 57 (1993) 491–497.

[4] M. Schulz, J. Sauerwald, H. Seh, H. Fritze and H. L. Tuller, "Defect chemistry based design of monolithic langasite structures for high temperature sensors", Solid State Ion., 184 (2011) 78–82. doi:10.1016/j.ssi.2010.08.009

[5] H. Habuka and Y. Tanaka, "In-situ monitoring of chemical vapor deposition from trichlorosilane gas and monomethylsilane gas using langasite crystal microbalance", ECS J. Solid State Sci. Technol., 1 (2012) 62–65. doi:10.4236/jsemat.2013.31A009

[6] H. Habuka and Y. Tanaka, "Langasite crystal microbalance frequency behavior over wide gas phase conditions for chemical vapor deposition", J. Surf. Eng. Mater. Adv. Technol., 3 (2013) 61–66. doi:10.1016/j.surfcoat.2013.06.052

[7] H. Habuka and M. Matsui, "Langasite crystal microbalance frequency behavior over wide gas phase conditions for chemical vapor deposition", Surf. Coat. Technol., 230 (2013) 312–315. doi:10.1016/j.surfcoat.2013.06.052

[8] H. Fritze, "High-temperature piezoelectric crystals and devices", J. Electroceram., 26 (2011) 122–161. doi:10.1007/s10832-011-9639-6

[9] K. K. Kanazawa and J. G. Gordon II, "The oscillation frequency of a quartz resonator in contact with liquid", Anal. Chim. Acta, 175 (1985) 99–105. doi:10.1016/S0003-2670(00)82721-X

[10] R. C. Reid, J. M. Prausnitz and B. E. Poling, The properties of gases and liquids, 4 ed. (McGraw-Hill, New York, 1987).

[11] P. Pollard and J. Newman, "Silicon deposition on a rotating disk", J. Electrochem. Soc., 127 (1980) 744–752. doi:10.1149/1.2129589

[12] H. Habuka, M. Matsui and A. Saito, 17th International Conference on Crystal Growth and Epitaxy, Proc. pp. 182–186 (Warsaw, Poland, 2013).

[13] H. Habuka and K. Kote, "Langasite crystal microbalance for development of reactive surface preparation of silicon carbide film deposition from monomethylsilane gas", Jpn. J. Appl. Phys., 50 (2011) 096505-1-4. doi:10.1143/JJAP.50.096505

[14] A. Saito, K. Miyazaki, M. Matsui and H. Habuka, "In-situ observation of chemical vapor deposition using $SiHCl_3$ and BCl_3 gases", Phys. Status Solidi C, 12 (2015) 953–957. doi: 10.1002/pssc.201510002

[15] G. Sauerbrey, "Verwendung von Schwingquarzen zur Wägung dünner Schichten und zur Mikrowägung", Zeitschrift fur Physik, 155 (1959) 206–222.

[16] H. Habuka, T. Nagoya, M. Mayusumi, M. Katayama, M. Shimada and K. Okuyama, "Model on transport phenomena and epitaxial growth of silicon thin film in $SiHCl_3$–H_2 system under atmospheric pressure", J. Cryst. Growth, 169 (1996) 61. doi: 10.1016/0022-0248(96)00376-4

[17] K. Miyazaki, A. Saito and H. Habuka, "In situ measurement for evaluating temperature change related to silicon film formation in a $SiHCl_3$–H_2 system", ECS J. Solid State Sci. Technol., 5 (2016) P16–P20. doi:10.1149/2.0101602jss

[18] D. Shen, H. Zhang, Q. Kang, H. Zhang and D. Yuan, "Oscillating frequency response of a langasite crystal microbalance in liquid phases", Sens. Actuators B, 119 (2006) 99–104. doi:10.1016/j.snb.2005.12.001

[19] D. Crippa, D. L. Rode and M. Masi, Silicon epitaxy (Academic Press, New York, 2001).

IntechOpen